



Typology of flood trends across West Africa

Gabrielle Sorini¹, Juliette Blanchet¹, G r my Panthou¹, Th o Vischel¹, and Yves Tramblay²

¹Univ. Grenoble Alpes, CNRS, INRAE, IRD, Grenoble INP, IGE, 38000 Grenoble, France

²Espace Dev, Univ. Montpellier, IRD, Montpellier, France

Correspondence: Gabrielle Sorini (gabrielle.sorini@univ-grenoble-alpes.fr)

Abstract

West Africa is a region highly vulnerable to global change, where hydro-climatic extremes become increasingly frequent and intense. While previous floods studies have been limited to few river basins with scattered observational data, the availability of a recent regional hydrometric in-situ database offers the opportunity for studying hydrological extremes at the west African scale. This study investigates trends in hydrological extremes using annual maximum streamflow (AMAX) over 80 West African catchments from 1950 to 2018. A rigorous flood frequency framework based on Extreme Value Theory is used for trends detection in return levels, comparing a wide variety of non stationary models. In order to synthesize the regional patterns, an objective typology of flood evolution trajectories is developed using k-means clustering. The results reveal widespread non-stationarity in flood extremes, affecting 85% of the catchments, with contrasted trajectories of extremes. The clustering reveal 6 main types of trends in hydrological extremes. While most catchments exhibit a general decline in flood magnitude until the major droughts affecting the region (1970s-1990s), recent decades show divergent evolutions, ranging from stabilization to moderate or strong increase. At the regional scale, a north-south gradient emerges. The Sahelian catchments display trajectories ranging from persistent decreases to weak flood intensification, whereas the Sudano-Guinean basins are predominantly characterized by decreasing trends, with additional nuances related to the shape and magnitude of these declines. Overall, these results challenge the assumption of an homogeneous signal of hydrological intensification over West Africa and provide a more nuanced depiction of typical Sahelian and Sudano-Guinean flood evolution patterns. Furthermore the contrasted trends identified are only weakly explained by catchment physical or hydrological characteristics, underscoring the complexity of non-stationary hydrological dynamics in the region. By documenting the diversity of long-term flood trajectories over 1950-2018, this study refines the regional narrative of hydrological changes in West Africa and has important implications for anticipating future hydro-climatic extremes and for supporting the strengthening of resilience of ecosystems and societies.

1 Introduction

West Africa is a tropical region that is particularly vulnerable to global changes. Its climate is extremely sensitive to climate change, as it is largely influenced by the West African monsoon (Lebel and Vischel, 2005). In recent years, the region has experienced unprecedented shifts, beginning with generalized warming, which alters monsoon dynamics and consequently



25 modifies rainfall intensity, occurrence and timing (Nicholson, 2013; Panthou et al., 2014; Taylor et al., 2017; Panthou et al.,
2018; Biasutti, 2019; Chagnaud et al., 2023; Spät et al., 2025). These major shifts have direct consequences for water resources
(Descroix et al., 2018; Cuthbert et al., 2019), rain-fed agricultural production, and challenge the adaptability of population and
ecosystems (Tschakert, 2007; Lalou et al., 2019). They occur against the backdrop of fast and interconnected transformation
in West Africa, with respect to climate, demography, and land-use changes, notably cropland expansion and increasing ur-
banization (OECD/SWAC, 2009; OSS, 2018; Birkmann et al., 2022; Trisos et al., 2022). Within this context, ecosystems and
populations are already coping with climate variability. In response to these combined climatic and socio-economic pressure,
ecosystems and societies in West Africa are developing various adaptation strategies (Tambol et al., 2025). Local knowledge
plays a key role in the development of practices aimed at facing rainfall variability, particularly changes in the timing of the
rainy season onset (Mendes et al., 2025). The observed increase in vegetative cover in some regions, together with the diver-
sification of agricultural practices to improve production, is often interpreted as evidence of resilience of both populations and
ecosystems (Descroix et al., 2024).

However, this resilience may be increasingly challenged by the growing frequency and intensity of climate extremes. Indeed,
in recent years, the region has frequently experienced hydro-climatic extremes, both wet and dry (Panthou et al., 2014; Taylor
et al., 2017; Panthou et al., 2018; Wilcox et al., 2018). Floods are among the most damaging and deadliest of these hydro-
climatic extremes, ranking among the most significant disasters in West Africa (Tramblay et al., 2020; Jonkman et al., 2024).
The number of people affected by floods has grown exponentially in recent decades (Aich et al., 2016; Birkmann et al., 2022).
Faced with this increase in damages, hydrological risk managers are often ill-equipped to incorporate the intensification of
hydrological hazards into their adaptation strategies. In particular, structural approaches to hydrological risk management are
challenged by the difficulty of designing infrastructure capable of ensuring the protection of people and assets in a context of
increasing hydrological hazard intensity (Milly et al., 2008; CEDEAO, 2020). In West Africa, the methods commonly used for
the hydrological design of flood protection structures are based on approaches developed from observations prior to 1970 and
rely on the assumption of hydrological stationarity (Amani and Paturel, 2017). These methods have now become obsolete, and
their application entails a significant risk of leading to inappropriate or inadequate sizing of hydraulic structures.

Robust information on the evolution of hydrological extremes and the associated mechanisms could be thus a great assistance
for supporting the ongoing resilience of population and ecosystems. There is therefore a growing scientific interest in improving
the detection of potential trends in floods across hydrological systems in West Africa, identifying possible regional or sub-
regional coherences, and assessing whether typologies of trends can be established. Such analyses constitute an important
prerequisite for identifying the mechanisms driving changes in extreme hydrological regimes, in relation to climate and land-
use changes, and as a function of the intrinsic hydromorphological characteristics of catchments in the region (Aich et al.,
2015; Descroix et al., 2018).

However, in West Africa, data scarcity and limited data accessibility constrain the number of studies addressing the evolution
of hydrological extremes over recent decades (Tramblay et al., 2021a). Most existing studies investigate extremes and their
temporal changes over a limited number of catchments. Some focus on major tributaries within large river systems such as the
Niger River (Aich et al., 2015; Wilcox et al., 2018; Massazza et al., 2021; Sauzedde et al., 2025) or the Senegal River (Diop



60 et al., 2017; Wilcox et al., 2018; Bruckmann et al., 2022), while others aim to document multiple catchments spread over the region across different basin scales and hydro-climatic contexts (Nka et al., 2015; Bossa et al., 2023). In the large basins of the Senegal River and the Sahelian Niger River studies indicate a tendency toward flood intensification since the 1990s. (Aich et al., 2015; Wilcox et al., 2018; Massazza et al., 2021; Sauzedde et al., 2025). The diversity of the catchments analyzed also shows that some basins in the region do not exhibit such intensification and that, when a trend exists, it can take various forms, including linear trends, multi-linear trends, or abrupt shifts (Nka et al., 2015; Wilcox et al., 2018; Bossa et al., 2023; Sauzedde et al., 2025).

At present, the ability to identify regional coherence in flood evolution or to derive typologies of trends remains limited by the spatial dispersion of the studied areas and by the diversity of methodological approaches adopted. The only notable exception to date providing a regional perspective on flood evolution is the study by Diop et al. (2025b). Their work builds on a comprehensive hydrological database for West Africa compiled by Trambly et al. (2021a), from which a regional flood frequency analysis was conducted at the West African scale. This analysis was first carried out under stationarity assumptions by comparing several statistical distributions of extremes, and was then extended to a non-stationary framework by assuming a linear evolution of return levels with no change in variability. Although regional in scope and methodologically consistent, this study did not reveal any clear regional coherence or specific typology of flood trends across the region. Our hypothesis is that the diversity of flood trend patterns documented in the literature across dispersed hydrosystems cannot be adequately represented solely by a linear evolution of return levels. In contrast with previous studies worldwide on trends in extreme precipitation (Ouarda and Charron, 2019; Jayaweera et al., 2025), extreme value models allowing for complex trends in return levels (e.g. non-linearity, change in variability...) have been only very sparsely explored so far for hydrological trends on floods, and even less so in Africa, probably due to the data scarcity and limited data accessibility already mentioned.

80 This paper aims to provide a systematic and coherent overview of flood trends at the scale of West Africa. The analysis covers the period 1950–2018 and is based on the database compiled by Trambly et al. (2021a). The study substantially extends the work of Diop et al. (2025b) in several key aspects: i) trend detection accounts for a wide diversity of temporal patterns affecting both the mean and variance of extremes; ii) it seeks to identify coherent typologies of flood trends; and iii) it explores potential links between these typologies and physical and morphological descriptors.

85 2 Region and data

2.1 Region

West Africa extends between 5° N – 20° N and 10° W – 20° E and encompasses a wide range of climatic and ecological environments (Figure 1). The northern part of the region includes the Sahel, a transition zone between the Sahara Desert and the savanna to the south. Further south lies Sudan, another ecological transition belt leading toward the tropical forests that characterize the Gulf of Guinea countries along the southern coast (OSS, 2018). The region experiences strong seasonality driven by the West African Monsoon. During boreal summer (May–September), moist southwesterly winds from the Gulf of Guinea migrate northward and interact with hot, dry Saharan air masses, generating monsoon rainfall. The withdrawal of

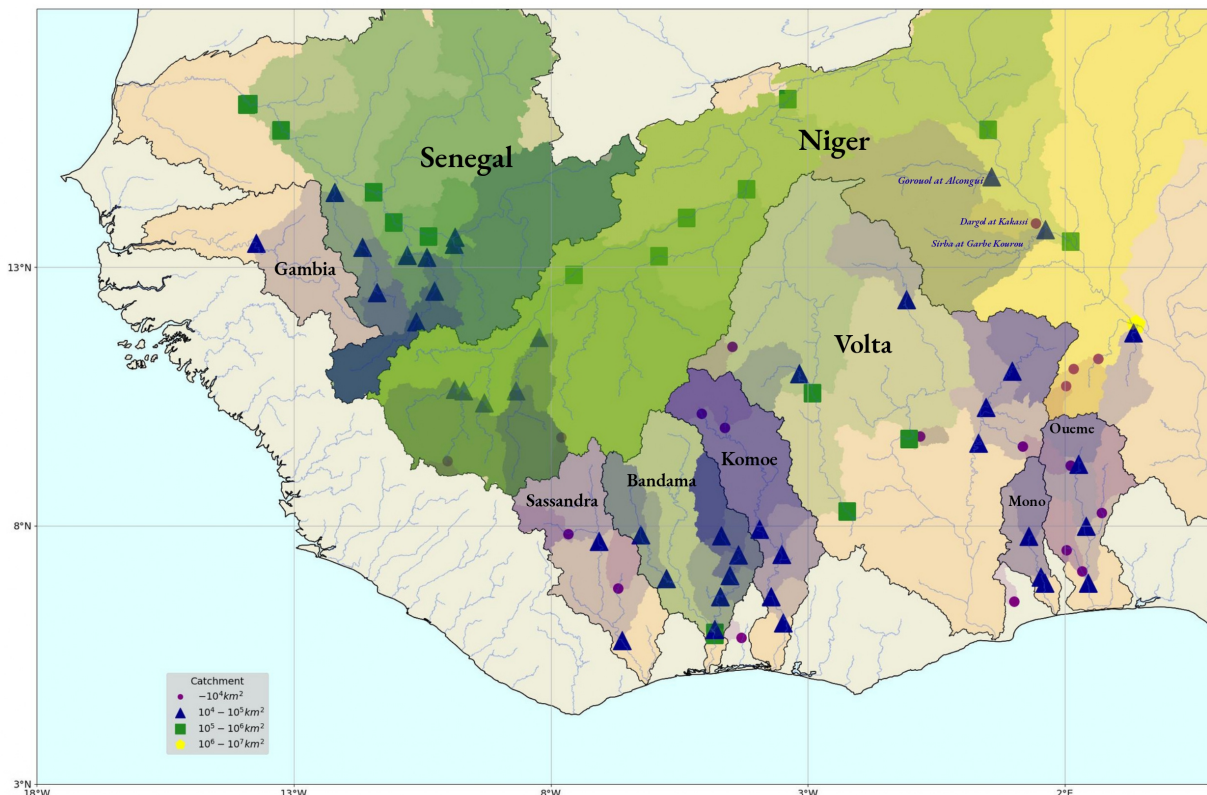


Figure 1. Location and delimitation of the main river basins covering West Africa. The 80 hydrometric stations used for the study are shown with specific symbols according to their catchment size. The corresponding catchments are delineated and colored. The sub-basins overlap, hence the different shades on the figure.

humid air southward marks the return of the dry season (Calvin et al., 2023). This monsoon system underpins West Africa’s marked climatic gradient—from the semi-arid Sahelian zone, to the Sudanian savannas, and finally to the humid tropical forests in the south. Over the past decades, West Africa has undergone significant shifts in rainfall regimes. The Sahel experienced wet conditions in the 1950s–1960s, followed by severe droughts in the 1970s–1980s. Since the 1990s, rainfall has generally increased, though with strong regional contrasts across the Sahel and surrounding zones (Panthou et al., 2018; Lebel and Ali, 2009). These climatic and ecological contrasts also shape hydrological behavior. Two main hydrological behaviors are usually distinguished in the literature. Sahelian basins largely exhibit Hortonian overland flow: runoff is produced once rainfall exceeds the soil’s infiltration capacity, making streamflow highly sensitive to surface soil properties and rainfall intensity (Horton, 1933). During the drought period (1970–1990), these basins showed an increase in runoff coefficients (Descroix et al., 2012). In contrast, Sudano-Guinean catchments feature predominantly Hewlettian processes, with both surface and subsurface flows contributing to streamflow due to higher soil hydraulic conductivity (Hewlett and Hibbert, 1967). These basins generally



105 exhibited a decrease in runoff coefficients during the same drought period (Descroix et al., 2012). Although differences in the dominant runoff-generation processes between the Sahelian and Sudano–Guinean zones have been linked to contrasting hydrological responses, particularly during the drought period, there is as yet no clear evidence of a coherent regional pattern in the evolution of extreme hydrological regimes.

2.2 Data

The data used for the study are time series of daily discharges extracted from the African Database of Hydrometric Indices (ADHI) (Tramblay et al., 2021a). This database combines hydro-climatological data from the GRDC (Global Runoff Data Center) and SIEREM (Système d’Information Environnementales sur les Ressources en Eaux en Afrique pour leur Modélisation) databases. A total of 395 hydrometric stations are deployed across West Africa, with a recording period between 1950 and 2018. To extend the temporal coverage of the dataset, time series from hydrometric stations located in the Niger River basin and its tributaries near Niamey (the Gorouol, Dargol and Sirba rivers), as compiled and documented by Sauzedde et al. (2025), were incorporated into the analysis.

A “flood season” is defined for each station as the period of the year encompassing the climatological peak of the hydrograph. An automatic peak detection procedure is applied using SciPy’s *find_peaks* function, based on two criteria: (i) a minimum peak width of 45 days, and (ii) a sufficient relative peak height. A manual inspection of flood peak timing and seasonality was performed to fine-tune the detection criteria and ensure a robust identification of the flood season. The start and end dates of the flood season are defined as the beginning and end of the detected peak width, using the *left_ips* and *right_ips* values returned by the algorithm. For most stations, the hydrograph displays a unimodal seasonal pattern (one peak). In cases where bimodality (two peaks) is identified, the flood season window is defined so as to encompass both peaks. In such cases, the second peak occurs before the hydrograph returns to baseflow conditions, indicating that both peaks belong to the same flood season. The annual maximum discharge over the hydrological year was then extracted for each station. The maximum is considered valid when the proportion of missing data within the flood season does not exceed 10%, otherwise it is tagged as nonvalid and considered missing. After this extraction of the AMAX series, only series with i) a minimum of 35 years of data, ii) no more than seven consecutive years of missing data and iii) at least 10 years of observations before and after 1980 were selected. These selection criteria ensure that all AMAX series include the severe drought periods experienced in the region from 1970 to 1990. All in all, this lead to select 80 AMAX series which are used in the present analysis.

130 From 1976 to 1987, approximately 60% of the 395 hydrometric stations provided valid annual maxima. After that period, the number of valid maxima dropped sharply—from about 60% to 30% in less than a decade. As a result, time series extending into recent decades are relatively scarce but remain sufficiently well distributed regionally so as not to undermine the proposed regional typological analysis.



3 Methodology

135 The general methodology consists of using an Extreme Value Theory framework to estimate trends in return levels by comparing a wide range of nonstationary models, and then classifying these trends to analyze the dominant patterns across the region. This methodological approach is generic and can be replicated in other regions, provided that sufficiently long observation series are available.

3.1 Detection of quantitative trends

140 The first step is to detect quantitative trends in each AMAX series. This section describes a rigorous framework based on flood frequency analysis for this purpose.

3.1.1 General framework of Extreme Value Theory

Frequency analysis is a statistical method of prediction. It involves learning from past events the probability that an event will not exceed a specified value x , which is represented by the cumulative distribution function (CDF) $F(x) = \mathbb{P}(X \leq x)$. The probability of exceedance is defined as $p(x) = 1 - F(x)$. This can be expressed as the return period $T(x) = 1/p(x)$, which is widely used in hydrological science. Equivalently, the T-year return level is defined as the value x such that $p(x) = 1/T$, i.e. $x = F^{-1}(1 - 1/T)$ where F^{-1} is the quantile function. In particular, the 2-year return level is the threshold expected to be exceeded on average once every two years.

Following Extreme Value Theory (Coles, 2001), annual maximum discharges are assumed to follow a Generalized Extreme Value distribution in both stationary and non-stationary contexts. First, a stationary GEV distribution is fitted to the AMAX series for each station. The stationary hypothesis assumes that the three parameters remain constant over time: $Q_{max} \sim GEV(\mu, \sigma, \xi)$ where μ is the location parameter modeling the bulk of the distribution, $\sigma > 0$ the scale parameter modeling the variability of the extremes and ξ the shape parameter governing the 'tail' behavior. The CDF of the GEV distribution is defined as :

$$155 \quad F(x; \mu, \sigma, \xi) = \mathbb{P}(X \leq x) = \exp \left\{ - \left[1 + \xi \left(\frac{x - \mu}{\sigma} \right) \right]^{-\frac{1}{\xi}} \right\}, \quad (1)$$

for $\xi \neq 0$ and $1 + \xi \left(\frac{x - \mu}{\sigma} \right) > 0$.

The associated probability density function (PDF) is given by:

$$f(x; \mu, \sigma, \xi) = \frac{1}{\sigma} \left[1 + \xi \left(\frac{x - \mu}{\sigma} \right) \right]^{-1/\xi - 1} \exp \left\{ - \left[1 + \xi \left(\frac{x - \mu}{\sigma} \right) \right]^{-1/\xi} \right\}. \quad (2)$$

In the special case of the Gumbel distribution, which corresponds to $\xi = 0$, the CDF simplifies to:



160
$$F(x; \mu, \sigma, 0) = \exp\left(-\exp\left(\frac{\mu - x}{\sigma}\right)\right), \quad (3)$$

and the corresponding PDF becomes:

$$f(x; \mu, \sigma, 0) = \frac{1}{\sigma} \exp\left(\frac{\mu - x}{\sigma}\right) \exp\left(-\exp\left(\frac{\mu - x}{\sigma}\right)\right). \quad (4)$$

The T-year return level is then given by

$$rl_T = \begin{cases} \mu + \sigma(-\log(1 - 1/T))^{(-\xi)-1/\xi} & \text{for the GEV case,} \\ \mu - \sigma \log(-\log(1 - 1/T)) & \text{for the Gumbel case.} \end{cases} \quad (5)$$

165 3.1.2 Non-stationary models

In order to consider trends in extremes, a non-stationary approach is followed by allowing μ and σ to be time-varying, using the year as covariate. Past studies that have adopted this approach on hydrosystems in West Africa (Aich et al., 2015; Wilcox et al., 2018; Sauzedde et al., 2025) have shown that a wide variety of trends are possible for these two parameters. We therefore use a set of multi-linear trend and break functions to describe this variety of trends. In a first family of models, the location parameter μ is allowed to vary linearly with the years - decreasing and increasing trends that will be estimated automatically on the data (Linear, see Table 1). In a second family of models, μ is allowed to follow two different trends with a transitional year (to be estimated) around the 1970s/1980s (DoubleLinear, see Table 1). In a third family of models, μ is considered stationary before or after a transitional year to be estimated (SemiLinearBefore and SemiLinearAfter, see Table 1). Finally, in a fifth family of models, the change in μ is discontinuous (Breakpoint, see Table 1). This family models a radical change in discharge magnitudes. The break year, to be estimated, is imposed to be in the second third of the observed years. In all these models, the scale parameter σ is either stationary, or time-varying proportionally to μ with a factor of σ_1 ($\sigma(t) = \sigma_1 \times \mu(t)$, Models "+" in Table 1). This case allows considering a trend in σ without increasing the number of parameters compared to the stationary case since only σ_1 has to be estimated.

3.1.3 Selection of the best non-stationary model

180 Model estimation is done by maximum likelihood, giving thus one stationary GEV model and ten non-stationary GEV models for each AMAX series. To select the best model at a given station, we follow the procedure illustrated in Figure 2.

The selection procedure involves a statistical comparison using the likelihood ratio test. This test is applied when comparing two models that are nested within each other, i.e. when M_x is a particular case of M_y . For example, the stationary model is a special case of any non-stationary model of Table 1 (imposing the trend to be 0). Based on the ratio of the likelihoods of M_x



| Model | μ | μ shape | σ | σ shape | ξ | Degree of freedom |
|--|---|-------------|---|----------------|---------|-------------------|
| Linear Linear + | $\mu(t) = \mu_0 t + \mu_1$ | | $\sigma = \sigma_1$ $\sigma(t) = \sigma_1 \times \mu(t)$ | | ξ_0 | 4 |
| DoubleLinear DoubleLinear + | $\mu(t) = \begin{cases} \mu_0 t + \mu_1 & \text{if } t < t_0 \\ \mu_2 t + (\mu_0 - \mu_2)t_0 & \text{if } t \geq t_0 \end{cases}$ | | $\sigma = \sigma_1$ $\sigma(t) = \sigma_1 \times \mu(t)$ | | ξ_0 | 6 |
| SemiLinearBefore SemiLinearBefore + | $\mu(t) = \begin{cases} \mu_0 t + \mu_1 & \text{if } t < t_0 \\ \mu_0 t_0 + \mu_1 & \text{if } t \geq t_0 \end{cases}$ | | $\sigma = \sigma_1$ $\sigma(t) = \sigma_1 \times \mu(t)$ | | ξ_0 | 5 |
| SemiLinearAfter SemiLinearAfter + | $\mu(t) = \begin{cases} \mu_0 t_0 + \mu_1 & \text{if } t < t_0 \\ \mu_0 t + \mu_1 & \text{if } t \geq t_0 \end{cases}$ | | $\sigma = \sigma_1$ $\sigma(t) = \sigma_1 \times \mu(t)$ | | ξ_0 | 5 |
| Breakpoint Breakpoint + | $\mu(t) = \begin{cases} \mu_0 & \text{if } t < t_0 \\ \mu_1 & \text{if } t \geq t_0 \end{cases}$ | | $\sigma = \sigma_1$ $\sigma(t) = \sigma_1 \times \mu(t)$ | | ξ_0 | 5 |

Table 1. The families of non-stationary GEV models considered in this study.

185 and M_y , we either accept or reject (at a given level) the null hypothesis that M_x is the true model for the data. The p-value of the test depends on the difference in the degree of freedom (number of parameters) between the two models, hence it assesses whether adding more degrees of freedom is relevant for the data. More precisely, the Likelihood Ratio Test (LRT) is based on the statistics:

$$\text{LRT} = 2(\log \mathcal{L}_y - \log \mathcal{L}_x)$$

190 where \mathcal{L}_y is the log-likelihood of the more complex model, and \mathcal{L}_x is that of the simpler one. Under the null hypothesis that the data follow M_x , the statistics follows a χ^2 distribution with degrees of freedom equal to the difference in the number of parameters between the two models. The selection procedure is shown in Figure 2. It consists in two steps that is applied to each AMAX series separately:

1. Stationarity Test

195 All non-stationary models are compared to the stationary model with the Likelihood Ratio Test. If at least one non-stationary model rejects the null hypothesis of stationarity, we proceed to the selection among non-stationary models (see step 2.). Otherwise, the sample is considered stationary, and the stationary model is retained.

2. Comparison of non-stationary models

200 First, the best model between SemiLinearAfter and SemiLinearBefore is selected comparing their log-likelihood. The following models are embedded: the Linear, the SemiLinear (After and Before), and the DoubleLinear models. These

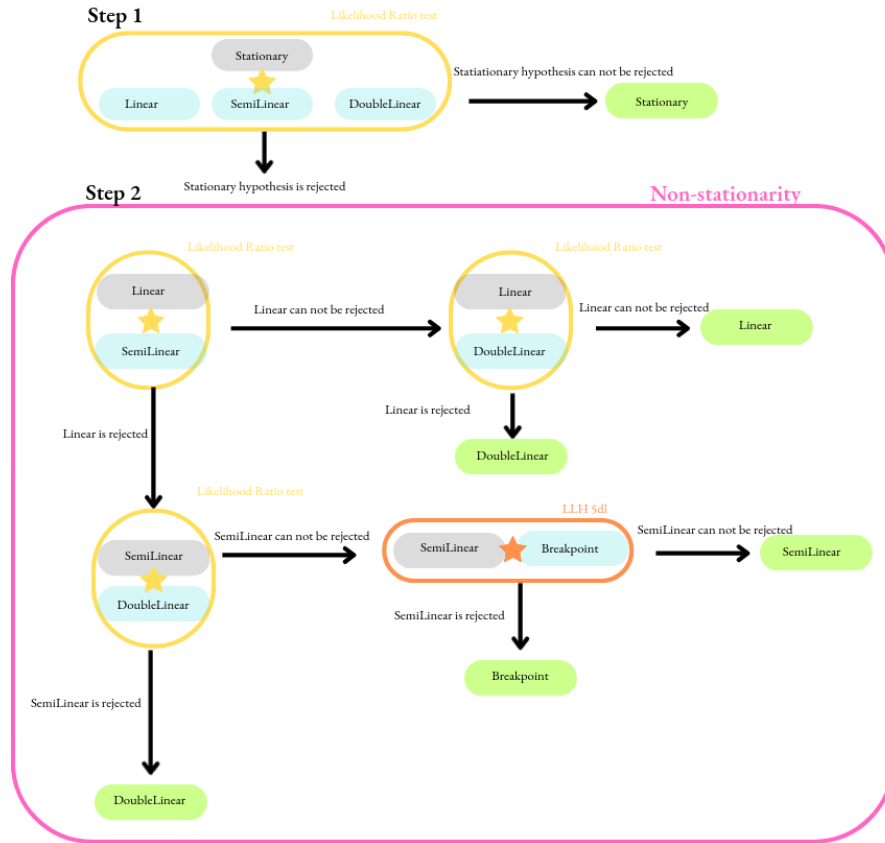


Figure 2. Chains of comparison for selection of the best model. The yellow circles indicate a comparison with the Likelihood Ratio Test. The orange circle indicates a direct comparison of log likelihood with the same degree of freedom. When a green model is reached in the comparison chain, this is the selected model.

models are compared pairwise using the Likelihood Ratio Test, following a chain of comparison shown in Figure 2. If the SemiLinear model is the best model at this step, we directly compare its log-likelihood to that of the (non embedded) Breakpoint model, as they have the same degrees of freedom.

This procedure is carried out in parallel in the following four cases in order to find the most parsimonious model:

- 205 – for the GEV distribution, with a stationary scale parameter (only the location parameter is allowed to vary);
- for the GEV distribution, with a non stationary scale parameter (both the location and scale parameters are allowed to vary);
- for the Gumbel distribution, with a stationary scale parameter (only the location parameter is allowed to vary);



– for the Gumbel distribution, with a non stationary scale parameter (both the location and scale parameters are allowed to vary).
210

The reason for considering both the GEV and the Gumbel distributions is that we look for the most parsimonious model and thus we allow for the possibility that a Gumbel model may be preferred due to its greater parcimony. The same reason explains why we also consider cases with a stationary scale parameter σ .

For each case, one model is selected following the procedure described above (Figure 2). Since the four selected models are not necessarily embedded, they are finally compared using the BIC, giving one best model per station. BIC is given by:
215

$$\text{BIC} = \log(n) \cdot k - 2 \log \mathcal{L}$$

where k is number of model parameters, n is the sample size and $\log \mathcal{L}$ is log-likelihood of the model. The final best model is that having the lowest BIC value.

Finally, for each station, the two-year return levels for the period from 1950 to 2020 are computed from this selected model using Eq. 5. The two-year return level is the threshold that is exceeded with a 50% probability each year. It is a fixed value in a stationary context, while it evolves over time in a non-stationary context. If the two-year return level increases over time, this indicates that an event with a 50% chance of being exceeded annually in the past has become more likely. In other words, rare events are becoming more frequent.
220

3.2 Classification of trends

A clustering analysis is used to build a classification of the quantitative trends in 2-year return levels. Note that the choice of a 2-year return level is arbitrary, and that the results would barely change with larger return levels, e.g. with the 10-year return level, since 2-year and 10-year return level functions are basically only shifted (unless $\sigma(t)$ shows a strong trend, which is never the case for our data). We use K-means, which is an unsupervised and iterative clustering algorithm allowing to objectively partition a dataset into K groups (or *clusters*) based on the data. Mathematically, K-means aims at minimizing the total within-cluster sum of squares. In this study, it is applied to classify the normalised vectors of 2-year return levels for the 1950–2020 period. Normalization is performed by dividing each 2-year return level by the station average return level between 1950 and 2020 (rl_2^{lim}).
230

$$rl_2^*(year) = \frac{rl_2(year)}{rl_2^{lim}} \quad (6)$$

Considering the vector of normalized 2-year return levels $rl_2^* = (rl_2^*(1950), \dots, rl_2^*(2020))$ for each station, K-means classifies the vectors (and hence the stations) into K groups whose centers C_1, \dots, C_K are given by the centroids of rl_2^* assigned to each cluster. To determine an optimal value of K , the silhouette method is used as a first guess. It is calculated for each station, as follows :

$$s(j) = \frac{b(j) - a(j)}{\max\{a(j), b(j)\}}, \quad (7)$$



where $a(j)$ is the average distance between the vector of rl_2^* for station j and the other vectors in the same cluster as j and $b(j)$ is the lower distance between the vector of rl_2^* for station j and the vectors in the other clusters. The silhouette score is then computed as the mean of the silhouette coefficients over all stations. The larger the silhouette, the better separated and grouped the clusters.

4 Results

4.1 Non stationarity in extreme floods

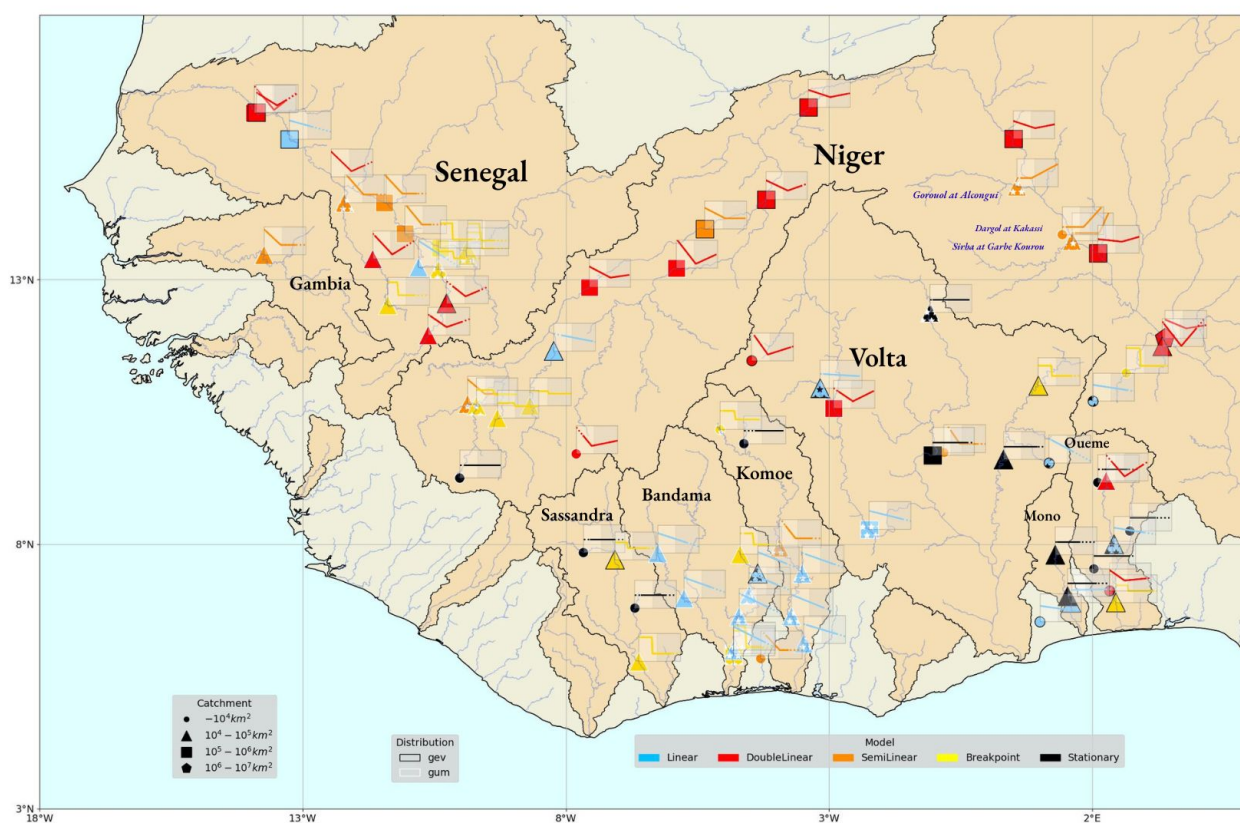


Figure 3. Map summarizing the selected models. The colors show the family of model selected. A window displays the two-year return level function between 1950 and 2020. The best distribution is outlined in black for the GEV distribution and in white for the Gumbel distribution. Stars inside the symbols indicate a time-varying σ .

Figure 3 shows the spatial distribution of the selected models and Table 2 their repartition among the six families of models.

The Gumbel distribution (65 %) is more often selected than the GEV distribution (35 %) in West Africa. The GEV distribution is selected for the Niger, Mono and Ouémé, and eastern Volta, and northern Senegal. The Gumbel distribution is largely



| Linear | DoubleLinear | SemiLinear | Breakpoint | Stationary |
|-----------------------|----------------------|--------------------|--------------------|------------|
| 20 (incl. 12 Linear+) | 19 (0 DoubleLinear+) | 12 (5 SemiLinear+) | 17 (6 BreakPoint+) | 12 |

Table 2. Repartition of the selected models among the six families of models for the 80 AMAX series.

selected in Sassandra, Bandama and Komoé, as well as in most parts of the Senegal basin and the upper Niger basin. Non stationarity reveals to be predominant with 85 % of non stationary AMAX series (see Table 2). The stationarity in AMAX
 250 serie is mostly found in the southern area (Figure 3). Among the non stationary models, 29 % of them allow non stationarity in the variability of extremes (scale parameter). The Linear model is selected in only 25 % of cases and is consistently associated with a downward trend. Notably, only 10 % of the stations select the simplest non-stationary model (Linear with stationary scale). More complex models thus largely dominate the overall selection. In particular, the DoubleLinear (24 %) and Breakpoint (21 %) models together account for nearly half of all cases. DoubleLinear models typically capture a marked
 255 shift from a decreasing trend to an increasing one, occurring around the 1980s. These patterns are mainly found in the northern part of West Africa. While the amplitude of the trends remains moderate in the Niger basin, the Senegal basin exhibits a much more pronounced V-shaped evolution. Similarly, Breakpoint models consistently indicate an abrupt decrease in annual maximum discharges, characterized by a transition from a high plateau to a lower one, again around the 1980s. SemiLinear models represent 15 % of the selected models and further refine this temporal change in trends. Most of them belong to the SemiLinear-
 260 Before category, featuring a downward trend followed by stabilization around the 1980s. In contrast, SemiLinearAfter models are rare and capture the onset of a positive trend after a prolonged stationary period, starting between the 1970s and 1990s. These models are selected for Gorouol, Darogol and Sirba rivers. At the regional scale, a clear zonal organization emerges. SemiLinear and DoubleLinear models are mainly concentrated in the northern Sahelian zone, especially within large basins such as the Senegal and Niger basins, whereas Stationary, Linear and Breakpoint models are more prevalent in the southern
 265 Sudano-Guinean region. Moreover, non-stationarity in the scale parameter is largely confined to the southernmost part of West Africa, while it remains predominantly stationary elsewhere. This indicates a greater interannual variability of floods in this region. Despite these coherent spatial patterns, a few series display atypical behaviors. In particular, small to medium-sized watersheds near Niamey show a strong post-1980 increase in maximum annual discharges (gray shaded area in Figure 3).

4.2 Classification of non stationary behaviors

270 The highest silhouette score is calculated for $K = 5$ clusters. Although this gives a first guess for the optimal K , it is important to look at the resulting clusters to insure consistency of the trends involved in each cluster. Examining the resulting five centroids revealed that one specific cluster was messy as it contained return levels functions showing distinct patterns, but clustered together because the trends were relatively small. To better distinguish these patterns, the choice was made to increase the number of clusters to six. This configuration yielded a silhouette score comparable to that of the five clusters solution. This

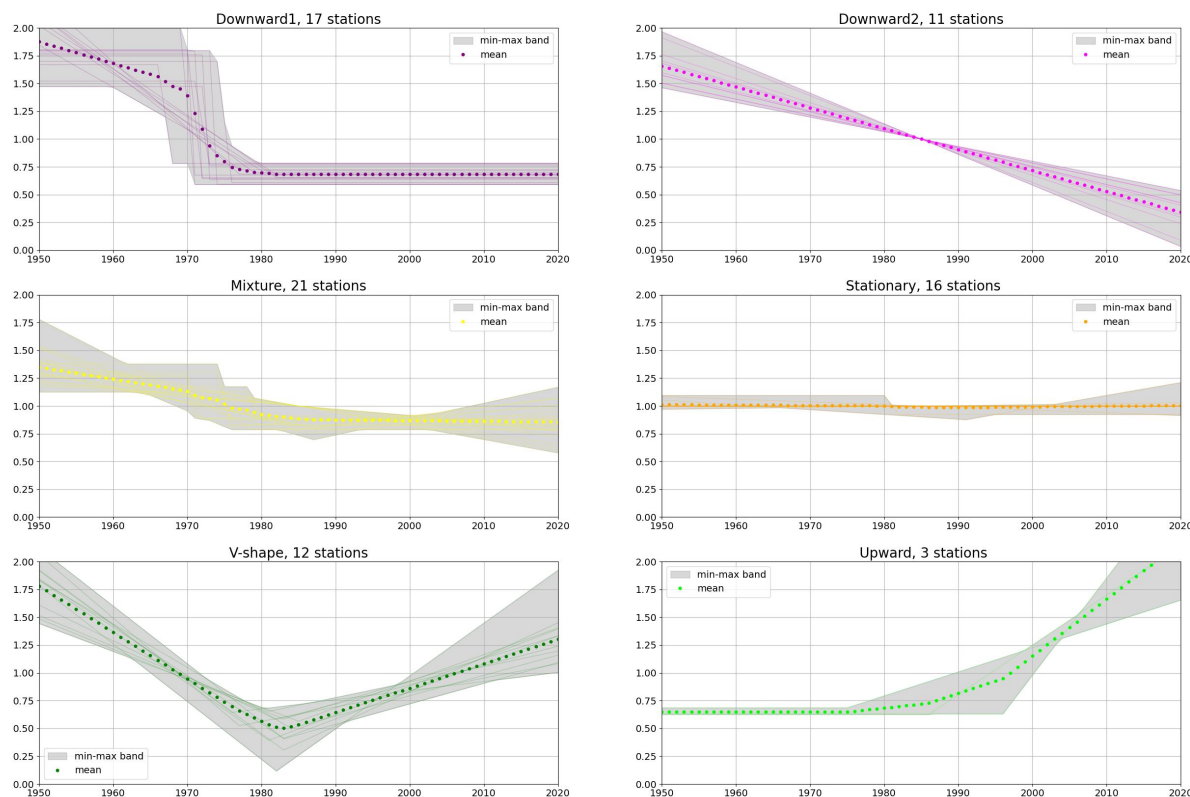


Figure 4. The 6 clusters of normalized 2-year return levels. The colored lines show the cluster centroids. The gray lines show the normalized 2-year return level function classified in each cluster.

275 choice of *six clusters* proved useful for having both distinct trends with underlying specific patterns, and interpretable centroids (see Figure 4).

The Upward cluster clearly stands out as it includes only 3 stations. Beside this exception, the clustering divides the stations into clusters of similar size (between 11 and 21 stations in each cluster). Except for the Stationary and Upward clusters, all clusters show a decline in return levels between the 1950s and the 1980s, but their evolution between the 1980s and the 2020s differs from cluster to cluster. The rate of decrease makes a key difference for the distinction of different types of trends and consequently for the clustering. The Stationary cluster regroups the cases of mere stationary extremes. Figure 5 shows that no spatial coherence is evident, except that the catchments associated tend to be located in the eastern part of the region. They are found in upstream Niger basin, and in a large watershed in the same river basin. They are also found in Sudano-Guinean

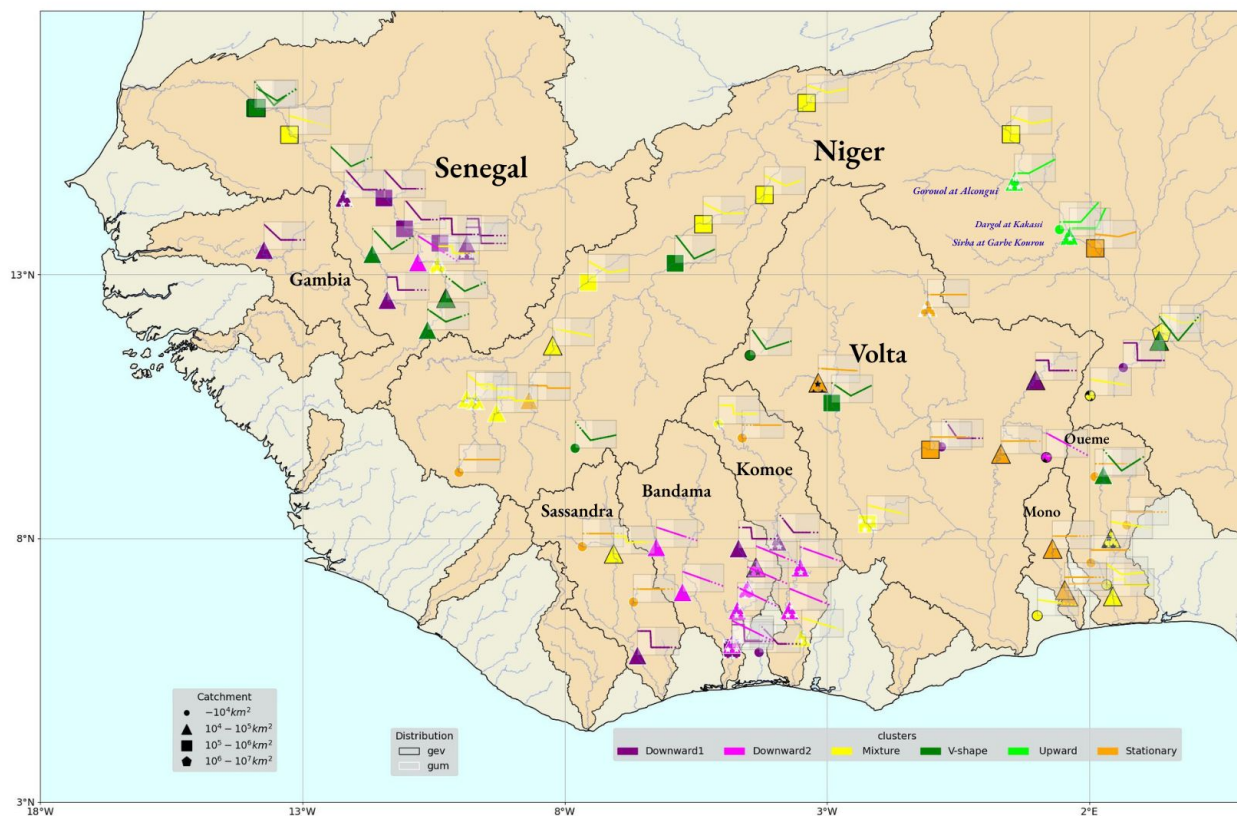


Figure 5. K-Means clustering results map. The colors indicate the cluster to which each catchment belongs. A window displays the two-year return level function between 1950 and 2020. The best statistical distribution is outlined in black for the GEV distribution and in white for the Gumbel distribution. Stars inside the symbols indicate a time-varying σ .

basins, with small to medium size catchments. A linear decline in 2-year return levels is exhibited in the Downward2 cluster and a sharp decline until the 1980s followed by a plateau in the Downward1 cluster. The corresponding catchments are located in similar areas, namely Bandama, Komoe, and central Senegal basin. These models exhibit a notable spatial coherence. A decrease followed by an increase in hydrological extremes is observed in the V-shape cluster. An increase in the recent period is also found in the Upward cluster, while extremes remain stationary in the first period, corresponding to SemiLinearAfter models. The catchments associated with these clusters are co-located in the northern part of the region. While the stations of the Upward cluster are located very close to each other on the tributaries of Niamey, no spatial coherence is observed for the stations associated with the V-shape cluster. Finally, the Mixture cluster includes the largest number of stations (21), with mixed patterns. The centroid shows a decline in extremes, followed by a stationary pattern. However different models (Breakpoint, SemiLinear and DoubleLinear) and thus different types of (mild) evolution are associated to this cluster (see the gray envelope in Figure 4). Most watersheds in the Niger basin belong to this cluster, which shows a slight increase from



295 upstream to downstream of the Niamey region. It also includes stations located in other river basins, which exhibit a slight downward trend.

4.3 Hydrological features behind clusters

In order to investigate the catchment features associated to each cluster, we consider 24 geomorphological, climatic and hydrological features listed in Table A1 in Appendix. Each catchment is represented by a vector of 24 feature values. Since the 300 features values have very different ranges, we normalize them between (0,1) by considering the percentiles they correspond to among the 80 catchments. By construction, the normalized features over the 80 catchments follow a uniform distribution. The question is then to know whether the distribution within a cluster differs significantly from the uniform distribution, in which case that feature can be hypothesized to play a role in the trends. Figure 6 shows the boxplots of the normalized features, together with the p-value of a Kolmogorov-Smirnov test against the uniform distribution.

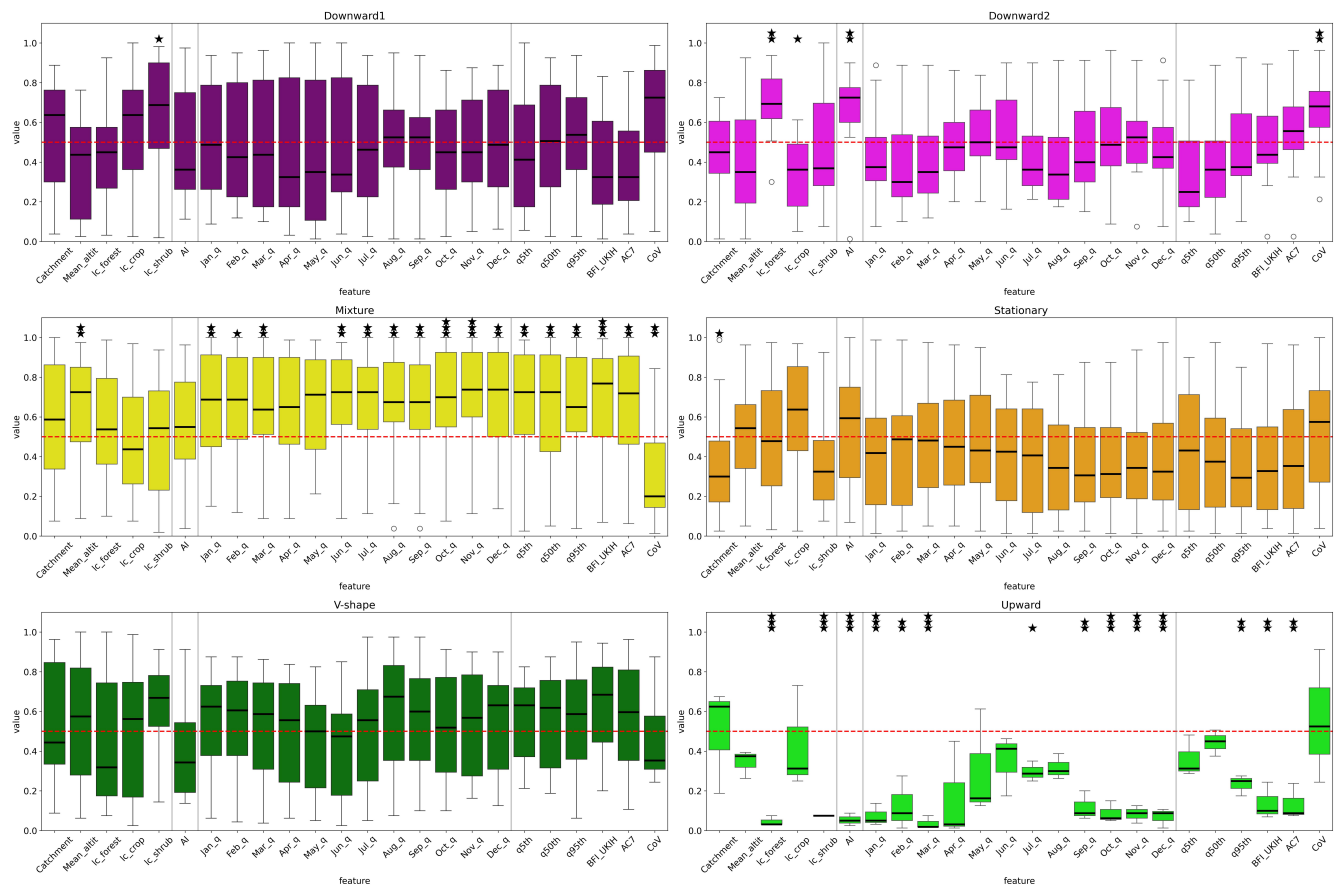


Figure 6. Distributions of the normalized catchment features inside each cluster. A star (respectively 2 and 3 stars) indicates when the test of uniform distribution has been rejected with a 10% (respectively 5% and 1%) significance level. The features are described in Appendix A.



305 The six clusters exhibit contrasted hydrological and geomorphological profiles, yet their interpretability for attribution re-
mains limited. Stationary behaviors (Cluster Stationary) correspond to the smallest and predominantly agricultural catchments,
with low baseflows and rapid hydrological response, whereas declining trends (Clusters Downward1 and Downward2) are
associated with basins showing relatively low baseflow and the highest relative flow variability. Catchments exhibiting a rise
in extremes after the 1980s (Cluster V-shape) tend to be small to medium systems in more arid regions, with sustained flows
310 and relatively low variability, while the mixed signals after the 1980s (Cluster Mixture) occurs in larger, high-altitude basins
characterised by high flows throughout the year and more pronounced relative variability. The small group showing increasing
trends (Cluster Upward) remains difficult to interpret due to the very limited number of catchments. Although some clusters
exhibit statistically discriminant features —particularly Cluster Mixture, and to a lesser extent Cluster Downward2 —, many
feature exhibit an approximately uniform distribution, making them only weakly discriminative.

315 5 Discussion

5.1 Hydrological behaviors in West Africa

5.1.1 Widespread but Diverse Flood Nonstationarity

Previous studies investigating hydrological extremes in West Africa have relied either on sparse datasets (Nka et al., 2015;
Wilcox et al., 2018) or on statistical approaches that constrained the range of admissible temporal evolutions, often limited
320 to monotonic (Diop et al., 2025b) or linear trends (Bossa et al., 2023). As a consequence, regional assessments of changes
in extreme floods have remained partial or potentially biased, either due to limited spatial coverage of gauging stations or
to modeling frameworks unable to capture complex temporal dynamics. By combining an extended spatial coverage with a
broader set of stationary and nonstationary models, our study enables a more comprehensive analysis.

As a result, our findings provide both a more coherent and nuanced picture of hydrological changes across West Africa. The
325 analysis confirms the predominance of nonstationarity in AMAX series at the regional scale. Nonstationary models outperform
stationary ones for a larger number of catchments than reported in previous studies (Nka et al., 2015; Aich et al., 2015; Wilcox
et al., 2018; Bossa et al., 2023), and concern a substantial proportion (85%) of the 80 hydrological series analyzed. Flood
nonstationarity since 1950 can therefore be considered a robust regional characteristic. Accounting for multi-linear temporal
evolution models further shows that simple linear trends (Diop et al., 2025b) or single-break models (Nka et al., 2015) alone
330 are insufficient to represent the diversity of flood evolution patterns observed in the region. This result is consistent with
geographically restricted studies by Aich et al. (2015) and Wilcox et al. (2018), which already pointed to the existence of more
complex dynamics. For the first time at the regional scale, we establish a typology of flood evolution patterns, highlighting
that certain temporal behaviors are consistent across multiple catchments and are sometimes associated with specific trend
directions. Linear and break-type patterns predominantly reflect decreasing trends over the study period, whereas double-
335 linear profiles most often indicate a decrease or near-stationarity of floods until the 1980s–1990s, followed by a subsequent
intensification.



5.1.2 Spatial organization of trends

The spatial coverage of the analyzed series, combined with the adopted trend analysis methodology and the classification of stations into trend typologies, enables the identification of a regional organization of hydrological trends. At first order, a pronounced south–north gradient in hydrological responses emerges. The Sudano–Guinean region is predominantly characterized by decreasing flood trends, occasionally interspersed with stationary or very weakly increasing behaviors. In contrast, the Sahelian zone is the only region exhibiting strong post-drought intensification patterns, although it also displays heterogeneous trajectories, with some catchments showing decreasing or moderately increasing trends. This organized regional perspective is novel and calls for a reassessment of the prevailing narrative of hydrological intensification in West Africa, which largely stems from the predominance of Sahelian catchments in previous studies. On the one hand, flood intensification appears to be almost exclusively confined to Sahelian basins, whereas catchments in the Sudano–Guinean zone predominantly exhibit decreasing flood magnitudes. Our results further reveal a marked diversity of flood evolution patterns within Sahelian basins, which also nuances the concept of hydrological intensification in the Sahel. In the Senegal River basin, some stations exhibit a recovery of hydrological extremes, in agreement with Wilcox et al. (2018). However, the inclusion of additional stations relative to Wilcox et al. (2018) reveals contrasting behaviors, including sharp and persistent decreases in extremes, thereby tempering the notion of a basin-wide flood intensification. In the Niger River basin, increasing trends are identified in specific tributaries such as the Gorouol, Sirba, and Dargol rivers. Nevertheless, the clustering analysis indicates that these increasing patterns are spatially confined to the vicinity of Niamey, while other sub-basins exhibit either no trend or only weak increases. While recent projections consistently suggest a positive evolution of flood magnitudes in future periods compared to 1985–2014, at an almost regional scale (Diop et al., 2025a), this study shows that such a signal has not yet clearly emerged in the observational records. Only in the Sahelian basins, the projected intensification may reflect a continuation of the already emerged historical trend. In contrast, marked inconsistencies are found between our observed trends and the projected changes in the Sudano–Guinean basins. These discrepancies may indicate a future trend that has not yet emerged from natural variability, or alternatively reflect limitations in the realism of the modeling chain used for projections related to atmospheric forcing, the representation of key atmospheric processes or their coupling. This calls for caution when interpreting future projections and raise broader questions regarding the extent to which future trends can be interpreted as a continuation of past behavior, particularly in the presence of potential breakpoints or regime shifts.

5.1.3 Hydrological Features and Trends

Our attempt to link catchment characteristics to the trend clusters identified in Section 4.3 did not reveal any clear attribution relationship. This result raises several points for discussion that cannot be conclusively addressed within the scope of the present study. The absence of a clear link may reflect the intrinsic difficulty of relating non-stationary hydrological behavior to stationary catchment attributes. The lack of temporal variability in the available descriptors likely contributes to this limitation, suggesting that nonstationary or time-varying catchment features may be more suitable for explaining divergent hydrological trajectories. Furthermore, the marked contrast in flood behavior between Sahelian and Sudano–Guinean basins



370 indicates that a deeper investigation of the mechanisms governing flood generation processes is warranted. Descroix et al.
(2009) suggested that this behavioral differentiation partly arises from the predominance of Hortonian runoff processes in the
Sahel, compared to Hewlettian (subsurface-dominated) processes in the Sudano–Guinean zone. In order to improve the attri-
bution of hydrological trends in the region, it therefore appears advisable to adopt approaches that explicitly distinguish the
dominant flood-generating processes and account for their temporal evolution, which may in some cases lead to persistent or
375 irreversible changes in hydrological behavior (e.g. Wendling et al., 2019). From a statistical perspective, complementary diag-
nostics could be considered, such as identifying groups of flood drivers that co-evolve and display coherent temporal dynamics
(Tramblay et al., 2021b, 2022). Such analyses may help reveal emerging non-stationarities and potential shifts in dominant
flood-generating mechanisms, thereby providing valuable insights into evolving hydrological behavior. While these quantita-
tive approaches constitute useful analytical tools to characterize the symptoms of changing flood-generating processes, full
380 attribution ultimately requires a deeper, process-based perspective.

5.2 Uncertainties and limitations

5.2.1 AMAX series

In analyzing extreme trends and their spatial distribution across West Africa, our study requires i) caution in selecting maxima
so as not to miss the true maxima, ii) ensuring that AMAX series are long enough to assess trends, iii) ensuring that stations are
385 well distributed across the region. The selection of a valid annual maximum is particularly important, given that missing values
during the flood season are critical. In our analysis, the selection of maxima was conducted under strict data quality criteria,
using SciPy's *find_peaks* function to identify flood season (see Section 2.2). Despite these precautions, residual uncertainties
remain, such as those related to measurement and observational errors. We have also applied strict criteria to ensure that AMAX
series are sufficiently long and numerous to enable trends to be estimated and their spatial distribution to be analyzed. These
390 criteria are i) the minimum number of years with data (set to 35), ii) the maximum number of consecutive years with missing
data (set to 7) and iii) the minimum number of years of observations before and after 1980 (set to 10). The criteria used enabled
us to select 80 stations, striking a balance between capturing as many annual maxima as possible to enable reliable estimation
of trends, and selecting a sufficient number of stations to study the spatial distribution of trends. However, using the AMAX
series has its limitations: by definition, it does not allow us to study the timing of hydrological extremes or the occurrence of
395 several large-scale events in the same year, as would be possible with an approach based on a peaks over threshold.

5.2.2 Model selection and covariates

Model selection among the four candidate models relied primarily on the BIC criterion. Comparing this with the AIC showed
strong, but not perfect, agreement: 85% consistency in choosing between the GEV and Gumbel distributions ; 90% consistency
in the chosen family model ; and 89% consistency in the type of variation of the scale parameter. These results suggest that
400 the model selection process is generally robust, while also highlighting its sensitivity to the chosen information criterion. Non-
stationarity was exclusively explored through temporal variations. However, previous studies have demonstrated the importance



of additional factors, such as precipitation and land use/land cover indicators, in explaining changes in hydrological extremes (Twinomuhangi et al., 2025). Incorporating these covariates could improve both our understanding and the accuracy of our models. This framework could also contribute to a more in-depth attribution analysis of hydrological trends. In addition, we have considered a variety of parametric models in order to adapt to different types of trends, but other behaviors may be present in the AMAX series (in particular non-linearity). There is here a tradeoff to find between what can be estimated from short time series (70 maxima at most) and having models that are not too strict to be able to capture different types of trends. More complex models, such as spline-based approaches, could also have been considered. However, these would introduce a large number of additional degrees of freedom. We therefore favor more parsimonious model.

410 5.2.3 Clustering analysis

Determining the optimal number of clusters requires balancing interpretability with the greater cohesion offered by a higher number of clusters. Statistical criteria do not necessarily converge towards a unique optimal value. Examining the resulting centroids with $K = 4, 5, 7$ and 8 clusters, the main typologies of hydrological extremes stand out, with additional nuanced separations emerging within individual clusters. Considering more than 6 clusters reduces the ability to identify coherent sub-regional patterns, while the catchment features are not found to be more discriminant (not shown). The non-stationarity of the features appears as a major limiting factor for the latter.

6 Conclusion

A rigorous framework for detecting quantitative trends in hydrological extremes was applied to 80 catchments across West Africa over the period 1950–2018. The availability of the ADHI in-situ database, which for the first time provides long and dense discharge records for a large number of stations in the region, made it possible to conduct a comprehensive and robust analysis of long-term hydrological trends. Non-stationarity was detected in 85% of the AMAX series, highlighting that non-stationary behavior constitutes a robust regional characteristic of hydrological extremes in West Africa. The analysis of trends in return levels reveals contrasting trajectories of hydrological evolution. A clustering approach allowed these trajectories to be grouped into six distinct types of flood trend patterns. Most clusters exhibit a general decrease in flood magnitudes from the 1950s until the major droughts that affected West Africa in the late 20th century. However, since the 1990s, the trajectories diverge markedly, with some clusters showing stabilisation while others display moderate to strong increasing trends. This first-time typology of flood evolution patterns refines the regional picture of hydrological change across West Africa. At the regional scale, a clear north–south gradient emerges, while substantial variability persists at finer spatial scales. Sahelian basins exhibit heterogeneous behaviours, whereas Sudano-Guinean catchments are predominantly characterised by decreasing trends. These findings challenge the previously assumed homogeneous signal of hydrological intensification over West Africa and provide greater granularity within the typical Sahelian and Sudano-Guinean hydrological evolution patterns. Within the Sahelian area, contrasted trajectories are identified, ranging from persisting decreasing trends to weak increases, and to pronounced flood intensification in specific areas, notably in tributaries of the Niamey region. In Sudano-Guinean basins, additional nuances



emerge, related to the linear or break-type patterns with respect to the magnitude of the decreasing trends. Overall, they
435 emphasise the complexity of hydrological dynamics in West Africa, which involves both regional and fine-scale dynamics.
The relationship between the identified clusters and catchment characteristics was further investigated. This analysis did not
reveal clear attribution pathways, nor did it allow the formulation of new attribution hypothesis based solely on climatic or
geomorphological descriptors. This highlights the limitations of traditional attribution approaches using only static parameters
to characterize the different trend typologies. It underscores the need to integrate non-stationary climatic drivers, land-use
440 and land-cover changes, as well as indicators of human influence into a more rigorous attribution framework. Advancing
attribution efforts in such a context remains considerably more complex than previously anticipated.

In the context of West African ecosystems and societies that are continuously adapting to strong hydro-climatic variability,
the contrasting hydrological evolutions identified here call for particular attention. Under ongoing global changes, these trends
may intensify, or shift, with important implications for water resources and risk management. Regular updates of such analyses
445 are therefore essential to better understand emerging hydro-climatic signals and to support the strengthening of resilience of
both populations and ecosystems in the face of future extremes.



Appendix A: Geomorphological, climatic and hydrological features

Table A1. The 24 geomorphological, climatic and hydrological features used to investigate the catchment features associated to each cluster, extracted from the ADHI database. The catchment area and mean altitude are computed using the HydroSHEDS database. The mean aridity index is extracted from CRU4, a widely used climate dataset. The hydrological indices are computed using the Toolbox for Streamflow Signatures in Hydrology (TOSSH). The baseflow index (BFI) is defined as the ratio of the baseflow volume to the streamflow volume. Baseflow is defined as the stable part of streamflow that is not directly caused by rainfall. The separation flow is calculated using the UK Institute of Hydrology method.

| Feature name | Descriptor |
|--------------------------------------|---|
| <i>Geomorphological features (5)</i> | |
| Catchment Area | Drainage basin area contributing to the station (km ²). |
| Mean Altitude | Average elevation of the catchment (m). |
| Forest cover | Percentage of catchment covered by forest. |
| Cropland | Percentage of catchment used as cropland. |
| Shrubland | Percentage covered by shrubs. |
| <i>Climatic feature (1)</i> | |
| AI | Mean aridity index |
| <i>Hydrological indices (18)</i> | |
| Jan_q | Mean streamflow for January (monthly mean in mm/s). |
| ... all months | ... all months |
| Dec_q | Mean streamflow for December (monthly mean in mm/s). |
| q5th | 5th percentile of daily streamflow distribution. |
| q50th | 50th percentile of daily streamflow (extreme high flows). |
| q95th | 95th percentile of daily streamflow (extreme high flows). |
| BFI_UKIH | Baseflow Index computed with UK Institute of Hydrology method (mm/s). |
| CoV | Coefficient of variation of runoff ($\frac{-std}{mean}$). |
| AC7 | Lag-7 autocorrelation of daily flow (weekly persistence). |

Author contributions. GS performed research, drafted the manuscript and made the figures. YT and GS cured and processed the datasets. JB, GP, TV proposed the initial ideas and designed the research. GS, JB, GP, TV discussed the results. All authors have proofread and revised the paper.

Competing interests. The authors declare no competing interest.

<https://doi.org/10.5194/egusphere-2026-1176>

Preprint. Discussion started: 2 April 2026

© Author(s) 2026. CC BY 4.0 License.



Acknowledgements. This study has received funding from Agence Nationale de la Recherche - France 2030 as part of the PEPR TRACCS programme under grant numbers ANR-22-EXTR-0005.



References

- 455 Aich, V., Liersch, S., Vetter, T., Andersson, J., Müller, E., and Hattermann, F.: Climate or Land Use? Attribution of Changes in River Flooding in the Sahel Zone, *Water*, 7, 2796–2820, 2015.
- Aich, V., Koné, B., Hattermann, F., and Paton, E.: Time Series Analysis of Floods across the Niger River Basin, *Water*, 8, 165, 2016.
- Amani, A. and Paturel, J.: Le projet de révision des normes hydrologiques en Afrique de l’Ouest et Afrique Centrale, *La Météorologie*, p. 6, 2017.
- 460 Biasutti, M.: Rainfall trends in the African Sahel: Characteristics, processes, and causes, 10, e591, <https://doi.org/10.1002/wcc.591>, 2019.
- Birkmann, J., Liwenga, E., Pandey, R., Boyd, E., Djalante, R., Gemenne, F., Leal Filho, W., Pinho, P., Stringer, L., and Wrathall, D.: Poverty, Livelihoods and Sustainable Development, in: *Climate Change 2022: Impacts, Adaptation and Vulnerability. Contribution of Working Group II to the Sixth Assessment Report of the Intergovernmental Panel on Climate Change*, edited by Pörtner, H.-O., Roberts, D., Tignor, M., Poloczanska, E., Mintenbeck, K., Alegría, A., Craig, M., Langsdorf, S., Löschke, S., Möller, V., Okem, A., and Rama, B., pp. 1171–1274, Cambridge University Press, Cambridge, UK and New York, NY, USA, <https://doi.org/10.1017/9781009325844.010>, 2022.
- 465 Bossa, A., Akpaca, J., Hounkpe, J., Yacouba, Y., and Badou, D.: Non-Stationary Flood Discharge Frequency Analysis in West Africa, 4, <https://doi.org/10.3390/geohazards4030018>, 2023.
- Bruckmann, L., Delbart, N., Descroix, L., and Bodian, A.: Recent hydrological evolutions of the Senegal River flood (West Africa), *Hydrological Sciences Journal*, 67, 385–400, <https://doi.org/10.1080/02626667.2021.1998511>, 2022.
- 470 Calvin, K., Dasgupta, D., Krinner, G., Mukherji, A., Thorne, P. W., Trisos, C., Romero, J., Aldunce, P., Barrett, K., Blanco, G., Cheung, W. W., Connors, S., Denton, F., Diongue-Niang, A., Dodman, D., Garschagen, M., Geden, O., Hayward, B., Jones, C., Jotzo, F., Krug, T., Lasco, R., Lee, Y.-Y., Masson-Delmotte, V., Meinshausen, M., Mintenbeck, K., Mokssit, A., Otto, F. E., Pathak, M., Pirani, A., Poloczanska, E., Pörtner, H.-O., Revi, A., Roberts, D. C., Roy, J., Ruane, A. C., Skea, J., Shukla, P. R., Slade, R., Slangen, A., Sokona, Y., Sörensson, A. A., Tignor, M., Van Vuuren, D., Wei, Y.-M., Winkler, H., Zhai, P., Zommers, Z., Hourcade, J.-C., Johnson, F. X., Pachauri, S., Simpson, N. P., Singh, C., Thomas, A., Totin, E., Arias, P., Bustamante, M., Elgizouli, I., Flato, G., Howden, M., Méndez-Vallejo, C., Pereira, J. J., Pichs-Madruga, R., Rose, S. K., Saheb, Y., Sánchez Rodríguez, R., Üрге-Vorsatz, D., Xiao, C., Yassaa, N., Alegría, A., Armour, K., Bednar-Friedl, B., Blok, K., Cissé, G., Dentener, F., Eriksen, S., Fischer, E., Garner, G., Guivarch, C., Haasnoot, M., Hansen, G., Hauser, M., Hawkins, E., Hermans, T., Kopp, R., Leprince-Ringuet, N., Lewis, J., Ley, D., Ludden, C., Niamir, L., Nicholls, Z., Some, S., Szopa, S., Trewin, B., Van Der Wijst, K.-I., Winter, G., Witting, M., Birt, A., Ha, M., Romero, J., Kim, J., Haites, E. F., Jung, Y., Stavins, R.,
- 480 Birt, A., Ha, M., Orendain, D. J. A., Ignon, L., Park, S., Park, Y., Reisinger, A., Cammaramo, D., Fischlin, A., Fuglestvedt, J. S., Hansen, G., Ludden, C., Masson-Delmotte, V., Matthews, J. R., Mintenbeck, K., Pirani, A., Poloczanska, E., Leprince-Ringuet, N., and Péan, C.: IPCC, 2023: Climate Change 2023: Synthesis Report. Contribution of Working Groups I, II and III to the Sixth Assessment Report of the Intergovernmental Panel on Climate Change [Core Writing Team, H. Lee and J. Romero (eds.)]. IPCC, Geneva, Switzerland., Tech. rep., Intergovernmental Panel on Climate Change (IPCC), <https://doi.org/10.59327/IPCC/AR6-9789291691647>, edition: First, 2023.
- 485 CEDEAO: Stratégie régionale de gestion des risques d’inondation, https://ecowas.int/?page_id=54213&lang=fr, 2020.
- Chagnaud, G., Panthou, G., Vischel, T., and Lebel, T.: Capturing and Attributing the Rainfall Regime Intensification in the West African Sahel with CMIP6 Models, *Journal of Climate*, 36, 1823–1843, <https://doi.org/10.1175/JCLI-D-22-0412.1>, 2023.
- Coles, S.: An introduction to statistical modeling of extreme values, Springer, London;New York, ISBN 978-1-85233-459-8, 2001.
- Cuthbert, M. O., Gleeson, T., Moosdorf, N., et al.: Global patterns and dynamics of climate–groundwater interactions, 9, 137–141, <https://doi.org/10.1038/s41558-018-0386-4>, 2019.
- 490



- Descroix, L., Mahé, G., Lebel, T., Favreau, G., Galle, S., Gautier, E., Olivry, J. C., Albergel, J., Amogu, O., Cappelaere, B., Dessouassi, R., Diedhiou, A., Le Breton, E., Mamadou, I., and Sighomnou, D.: Spatio-temporal variability of hydrological regimes around the boundaries between Sahelian and Sudanian areas of West Africa: A synthesis, *Journal of Hydrology*, 375, 90–102, 2009.
- Descroix, L., Genthon, P., Amogu, O., Rajot, J. L., Sighomnou, D., and Vauclin, M.: Change in Sahelian Rivers hydrograph: The case of recent red floods of the Niger River in the Niamey region, *Global and Planetary Change*, 98-99, 18–30, 2012.
- Descroix, L., Guichard, F., Grippa, M., Lambert, L., Panthou, G., Mahé, G., Gal, L., Dardel, C., Quantin, G., Kergoat, L., Bouaita, Y., Hiernaux, P., Vischel, T., Pellarin, T., Faty, B., Wilcox, C., Malam Abdou, M., Mamadou, I., Vandervaere, J.-P., Diongue-Niang, A., Ndiaye, O., Sané, Y., Dacosta, H., Gosset, M., Cassé, C., Sultan, B., Barry, A., Amogu, O., Nka Nnomo, B., Barry, A., and Paturel, J.-E.: Evolution of Surface Hydrology in the Sahelo-Sudanian Strip: An Updated Review, *Water*, 10, 748, 2018.
- Descroix, L., Luxereau, A., Lambert, L., Olivier, R., Diedhiou, A., Diongue-Niang, A., Dia, A., Fabrice, G., Manga, S., Diedhiou, A., Andrieu, J., Chevalier, P., and Faty, B.: An Interdisciplinary Approach to Understand the Resilience of Agrosystems in the Sahel and West Africa, *Sustainability*, 16, 5555, <https://doi.org/10.3390/su16135555>, 2024.
- Diop, A., Yaseen, Z. M., Bodian, A., Djaman, K., and Brown, L.: Trend analysis of streamflow with different time scales: A case study of the upper Senegal River, *ISH Journal of Hydraulic Engineering*, <https://doi.org/10.1080/09715010.2017.1333045>, 2017.
- Diop, S. B., Ekolu, J., Trambly, Y., Dieppoiss, B., Grimaldi, S., Bodian, A., Blanchet, J., Rameshwaran, P., Salamon, P., and Sultan, B.: Climate change impacts on floods in West Africa: new insight from two large-scale hydrological models, *Natural Hazards and Earth System Sciences*, 25, 3161–3184, 2025a.
- Diop, S. B., Trambly, Y., Bodian, A., Ekolu, J., Rouché, N., and Dieppoiss, B.: Flood Frequency Analysis in West Africa, *Journal of Flood Risk Management*, 18, <https://doi.org/10.1111/jfr3.70001>, 2025b.
- Hewlett, J. and Hibbert, A.: Factors affecting the response of small watersheds to precipitation in humid areas, *Forest hydrology*, pp. 275–290, 1967.
- Horton, R.: The role of infiltration in the hydrologic cycle, *Trans. Am. Geophys. Union*, 14, 446–460, 1933.
- Jayaweera, L., Wasko, C., and Nathan, R.: Evidence for non-stationarity in the GEV shape parameter when modeling extreme rainfall, *Water Resources Research*, 61, e2023WR036426, 2025.
- Jonkman, S., Curran, A., and Bouwer, L. M.: Floods have become less deadly: an analysis of global flood fatalities 1975–2022, *Natural Hazards*, 120, 6327–6342, 2024.
- Lalou, R., Sultan, B., Muller, B., et al.: Does climate opportunity facilitate smallholder farmers’ adaptive capacity in the Sahel?, 5, 81, <https://doi.org/10.1057/s41599-019-0288-8>, 2019.
- Lebel, T. and Ali, A.: Recent trends in the Central and Western Sahel rainfall regime (1990-2007), *Journal of Hydrology*, 375, 52–64, 2009.
- Lebel, T. and Vischel, T.: Climat et cycle de l’eau en zone tropicale : un problème d’échelle, *Comptes Rendus Geosciences*, 337, 29–38, 2005.
- Massazza, G., Bacci, M., Descroix, L., Ibrahim, M. H., Fiorillo, E., Katiellou, G. L., Panthou, G., Pezzoli, A., Rosso, M., Sauzedde, E., Terenziani, A., De Filippis, T., Rocchi, L., Burrone, S., Tiepolo, M., Vischel, T., and Tarchiani, V.: Recent Changes in Hydroclimatic Patterns over Medium Niger River Basins at the Origin of the 2020 Flood in Niamey (Niger), *Water*, 13, 1659, <https://doi.org/10.3390/w13121659>, 2021.
- Mendes, O., Correia, E., and Fragoso, M.: Variability and trends of the rainy season in West Africa with a special focus on Guinea-Bissau, 156, 15, <https://doi.org/10.1007/s00704-025-05471-6>, 2025.



- Milly, P. C. D., Betancourt, J., Falkenmark, M., Hirsch, R. M., Kundzewicz, Z. W., Lettenmaier, D. P., and Stouffer, R. J.: CLIMATE CHANGE: Stationarity Is Dead: Whither Water Management?, *Science*, 319, 573–574, 2008.
- 530 Nicholson, S.: The West African Sahel: A Review of Recent Studies on the Rainfall Regime and Its Interannual Variability, *ISRN Meteorology*, 2013, 1–32, 2013.
- Nka, B. N., Oudin, L., Karambiri, H., Paturel, J. E., and Ribstein, P.: Trends in floods in West Africa: analysis based on 11 catchments in the region, *Hydrology and Earth System Sciences*, 19, 4707–4719, 2015.
- OECD/SWAC: Regional Atlas on West Africa, *West African Studies*, OECD Publishing, Paris, <https://doi.org/10.1787/9789264056763-en>,
535 2009.
- OSS: Sahel et Afrique de l’Ouest – Atlas des cartes d’occupation du sol, Observatoire du Sahara et du Sahel (OSS), projet de renforcement de la résilience par le biais de services liés à l’innovation, la communication et aux connaissances (BRICKS) – Bénin, Burkina Faso, Éthiopie, Ghana, Mali, Mauritanie, Niger, Nigéria, Sénégal, Soudan, Tchad et Togo, 2018.
- Ouarda, T. B. and Charron, C.: Changes in the distribution of hydro-climatic extremes in a non-stationary framework, *Scientific Reports*, 9,
540 8104, 2019.
- Panthou, G., Vischel, T., Lebel, T., Quantin, G., and Molinié, G.: Characterising the space-time structure of rainfall in the Sahel with a view to estimating IDAF curves, *Hydrology and Earth System Sciences*, 18, 5093–5107, 2014.
- Panthou, G., Lebel, T., Vischel, T., Quantin, G., Sane, Y., Ba, A., Ndiaye, O., Diongue-Niang, A., and Diopkane, M.: Rainfall intensification in tropical semi-arid regions: the Sahelian case, *Environmental Research Letters*, 13, 064 013, 2018.
- 545 Sauzedde, E., Vischel, T., Panthou, G., Tarchiani, V., Massazza, G., and Housseini Ibrahim, M.: Compound-event analysis in non-stationary hydrological hazards: a case study of the Niger River in Niamey, *Hydrological Sciences Journal*, pp. 1–16, <https://doi.org/10.1080/02626667.2024.2435534>, 2025.
- Spät, D., Biasutti, M., and Voigt, A.: Extreme Sahelian Rainfall Continues to Rise Despite Stable Storm Frequency, 52, e2025GL115942, <https://doi.org/10.1029/2025GL115942>, 2025.
- 550 Tambol, T., Derbile, E., and Soulé, M.: Use of climate smart agriculture technologies in West Africa peri-urban Sahel in Niger, 15, <https://doi.org/10.1038/s41598-024-82813-w>, 2025.
- Taylor, C., Belusic, D., Guichard, F., Parker, D., Vischel, T., Bock, O., Harris, P., Janicot, S., Klein, C., and Panthou, G.: Frequency of extreme Sahelian storms tripled since 1982 in satellite observations, *Nature*, 544, 475–478, 2017.
- Tramblay, Y., Villarini, G., and Zhang, W.: Observed changes in flood hazard in Africa, *Environmental Research Letters*, 15, 1040b5,
555 <https://doi.org/10.1088/1748-9326/abb90b>, 2020.
- Tramblay, Y., Rouché, N., Paturel, J.-E., Mahé, G., Boyer, J.-F., Amoussou, E., Bodian, A., Dacosta, H., Dakhlaoui, H., Dezetter, A., Hughes, D., Hanich, L., Peugeot, C., Tshimanga, R., and Lachassagne, P.: ADHI: the African Database of Hydrometric Indices (1950–2018), 13, 1547–1560, <https://doi.org/10.5194/essd-13-1547-2021>, publisher: Copernicus GmbH, 2021a.
- Tramblay, Y., Villarini, G., El Khalki, E. M., Gründemann, G., and Hughes, D.: Evaluation of the drivers responsible for flooding in Africa,
560 *Water Resources Research*, 57, e2021WR029 595, 2021b.
- Tramblay, Y., Villarini, G., Saidi, M. E., Massari, C., and Stein, L.: Classification of flood-generating processes in Africa, *Scientific reports*, 12, 18 920, 2022.
- Trisos, C. H., Adelekan, I., Totin, E., Ayanlade, A., Efitre, J., Gameda, A., Kalaba, K., Lennard, C., Masao, C., Mgaya, Y., Ngaruiya, G., Olago, D., Simpson, N., and Zakieldean, S.: Africa, in: *Climate Change 2022: Impacts, Adaptation and Vulnerability. Contribution of Working Group II to the Sixth Assessment Report of the Intergovernmental Panel on Climate Change*, edited by Pörtner, H.-O., Roberts,
- 565



- D., Tignor, M., Poloczanska, E., Mintenbeck, K., Alegría, A., Craig, M., Langsdorf, S., Löschke, S., Möller, V., Okem, A., and Rama, B., pp. 1285–1455, Cambridge University Press, Cambridge, UK and New York, NY, USA, <https://doi.org/10.1017/9781009325844.01>, 2022.
- 570 Tschakert, P.: Views from the vulnerable: Understanding climatic and other stressors in the Sahel, 17, 381–396, <https://doi.org/10.1016/j.gloenvcha.2006.11.008>, 2007.
- Twinomuhangi, M. B., Bamutaze, Y., Kabenge, I., Wanyama, J., Kizza, M., Gabiri, G., and Egli, P. E.: Analysis of stationary and non-stationary hydrological extremes under a changing environment: A systematic review, 8, 332–350, <https://doi.org/10.1016/j.hydres.2024.12.007>, 2025.
- 575 Wendling, V., Peugeot, C., Mayor, A. G., Hiernaux, P., Mougin, E., Grippa, M., Kergoat, L., Walcker, R., Galle, S., and Lebel, T.: Drought-induced regime shift and resilience of a Sahelian ecohydrosystem, *Environmental Research Letters*, 14, 105 005, <https://doi.org/10.1088/1748-9326/ab3dde>, 2019.
- Wilcox, C., Vischel, T., Panthou, G., Bodian, A., Blanchet, J., Descroix, L., Quantin, G., Cassé, C., Tanimoun, B., and Kone, S.: Trends in hydrological extremes in the Senegal and Niger Rivers, *Journal of Hydrology*, 566, 531–545, 2018.